Effect of the Excitation Wavelength on the Ultrafast Charge Recombination Dynamics of Donor−Acceptor Complexes in Polar Solvents

Olivier Nicolet,[#] Natalie Banerji, Stéphane Pagès, and Eric Vauthey*

Department of Physical Chemistry, University of Geneva, 30 quai Ernest-Ansermet, CH-1211 Geneva, Switzerland

Received: June 15, 2005; In Final Form: July 19, 2005

The effect of the excitation wavelength on the charge recombination (CR) dynamics of several donor−acceptor complexes (DACs) composed of benzene derivatives as donors and of tetracyanoethylene or pyromellitic dianhydride as acceptors has been investigated in polar solvents using ultrafast time-resolved spectroscopy. Three different wavelength effects have been observed. (1) With complexes exhibiting two well-separated charge-transfer bands, the CR dynamics was found to be slower by a factor of about 1.5 upon excitation in the high-energy band. This effect was measured in both fast and slow relaxing solvents and was discussed in terms of different DAC geometries. (2) When the CR is faster than diffusive solvation, a slowing down of the CR with increasing excitation wavelength accompanied by an increase of the nonexponential character of the dynamics was measured. This effect appears only when exciting on the red edge of the charge-transfer absorption band. (3) When the driving force for CR is small, both nonequilibrium (hot) and thermally activated CR pathways can be operative. The results obtained with such a complex indicate that the relative contribution of these two paths depends on the excitation wavelength.

Introduction

For many practical applications, the charge recombination (CR) of ion pairs formed upon photoinduced electron-transfer (ET) reactions is an unwanted energy-wasting process. For this reason, the factors influencing its dynamics have been investigated in detail.[1−9] There are two major difficulties when studying the CR dynamics of an ion pair formed upon bimolecular ET. The first, which is still debated, concerns the exact nature of this ion pair, contact ion pair (CIP), or solvent-separated ion pair.[8−13] The second is that the time resolution of the measurements is limited to the time scale of ion pair formation. Thus, the CR dynamics is no longer experimentally accessible as soon as it is faster than quenching. Both problems can be eliminated when working with a donor−acceptor complex (DAC). Indeed, excitation in its charge-transfer (CT) band results in the population of an excited state that is essentially a CIP. The investigation of the CR dynamics of CIPs generated by CT excitation has been pioneered by Mataga and co-workers,[14−16] who have shown that its driving force dependence deviates substantially from the predictions of the semiclassical theory of nonadiabatic ET reaction, especially in the weakly exergonic region. While this theory predicts an increase of the rate constant with the driving force (normal regime) followed by a decrease at higher exergonicity (inverted regime),[17] only the inverted regime is observed with the CR of CIPs.[14−16,18] Indeed, CR becomes faster as the driving force decreases and takes place in the subpicosecond time scale at $\Delta G_{CR} > \sim -1$ eV. Several hypotheses have been proposed to explain this effect.[18−22] We have recently shown that the driving force, the solvent and the temperature dependence of the CR dynamics of a series of excited DACs composed of methoxybenzenes and pyromellitic dianhydride, could be very well reproduced with the hybrid model of Barbara and co-workers,[23,24] after incorporation of the contribution of inertial motion to solvation.[25] The basic idea of this model is illustrated in Figure 1: upon optical excitation, the excited DAC population is formed away from equilibrium and, therefore, CR can take place while the population is still relaxing as soon as the Franck−Condon factor is large enough. Of course, such a "hot" CR requires a sufficiently large electronic coupling constant, *V*. For weakly exergonic processes, CR can completely occur before the excited population has equilibrated, and the normal region where CR is a thermally activated process is not observed. An important signature of the nonequilibrium char-

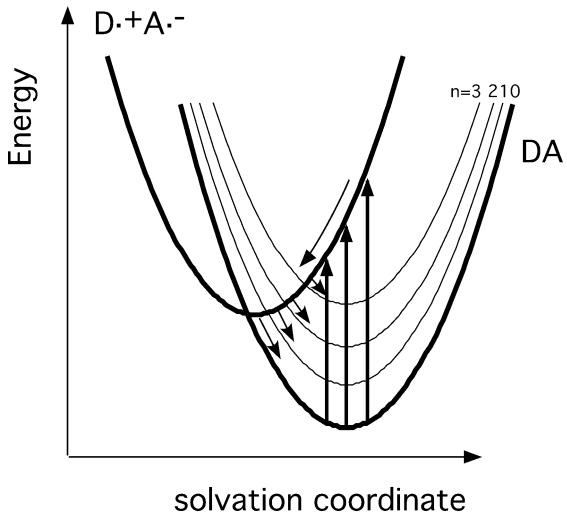

Figure 1. Cuts in the free energy surface of the ground and excited states of a DAC along the solvation coordinate illustrating the dependence of the nonequilibrium CR dynamics on the excitation wavelength. The thin parabolas represent vibrational excited states.

[#] Present address: Chemistry Division, Lawrence Berkeley National Laboratory, Berkeley, CA 94720-8198.
* Corresponding author: eric.vauthey@chiphy.unige.ch.

10.1021/jp0532216 CCC: $30.25
Published on Web 08/27/2005

TABLE 1: Static Dielectric Constant, ϵ_s, Viscosity, η, and Diffusional Solvation Time, τ_s, of the Solvents

solvent	ϵ_s[a]	η (cP)[a]	τ_s (ps)
ACN	37.5	0.345	0.50[b]
VaCN	19.7	0.693	4.7[c]
OcCN	13.9	1.64	6.4[c]

[a] Ref 39. [b] Ref 23. [c] Ref 40.

acter of ultrafast CR is that the decay dynamics of the CIP population is not exponential. Such nonexponential dynamics has not been firmly confirmed experimentally yet. There are indeed only a very few investigations of ultrafast (<1 ps) CR dynamics of excited DACs.[14,25,26] In the case of slower CR, the time profile of the CIP population can, in most cases, be reproduced with a biexponential function with one rising component, generally ascribed to structural changes within the CIP, and one decaying component associated with CR.[16,25] For faster CR, the time resolution and/or the signal-to-noise ratio of the data were not sufficient to exclude a nonexponential decay dynamics. It should also be mentioned that ultrafast CR dynamics has also been investigated by measuring the ground-state recovery dynamics of DACs.[27,28] As the primary CR product is the vibrationally hot electronic ground state, the bleach recovery dynamics is much more difficult to interpret than the decay of the CIP population, because of the entanglement of both CR and vibrational relaxation.

Another consequence of the nonequilibrium nature of CR is that the dynamics depends on how far from equilibrium the CIP state is initially populated. Therefore, the CIP population decay should depend on the excitation wavelength as shown in Figure 1. This has recently been confirmed by theoretical calculations of the CR dynamics of DACs using both the time-dependent perturbation theory and the stochastic-point transition approach.[29−31] The excited-state population decay was also calculated to be highly nonexponential. With the exception of very weakly exergonic CR ($\Delta G_{CR} > -0.4$ eV), the effective time constant of CR was found to increase with increasing excitation energy. It should be noted that in these calculations, the CT absorption band was assumed to be due to a single 0−0 transition. The reality is certainly more complex as it is well-known that in some cases, several CT transitions with similar frequencies contribute to the absorption band.[32−34] Similarly, resonance Raman measurements with DACs have shown the contributions of several Franck−Condon active vibrational modes to the CT transition.[35,36] Moreover, it has been recently suggested that "random donor−acceptor pairs", i.e., pairs with donor−acceptor distances larger than about 10 Å, also exhibit some absorption in the same region as the DACs.[37,38]

We report here on an experimental investigation of the effect of excitation wavelength on the ultrafast CR dynamics of various DACs in several polar solvents characterized by different dynamic properties (see Table 1). The effect of excitation in two distinct CT bands has first been studied. The effect of excitation wavelength within an absorption band due to either a single CT transition or two CT transitions with similar energies has then been measured with DACs composed of tetracyanoethylene, pyromellitic dianhydride, and tetracyanoquinodimethane as electron acceptors and series of methyl- and methoxybenzene derivatives as electron donors (see Chart 1). This allowed a free energy range for CR going from −0.9 to −1.6 eV to be explored. The more exergonic region was not investigated because, in this case, CR is slower than solvent relaxation and is thus not expected to exhibit nonequilibrium dynamics.

CHART 1. Electron Donors and Acceptors, and Redox Potentials in Acetonitrile (in V vs SCE; [a]Ref 9, [b] Ref 25, [c] Ref 18, [d] Ref 41)

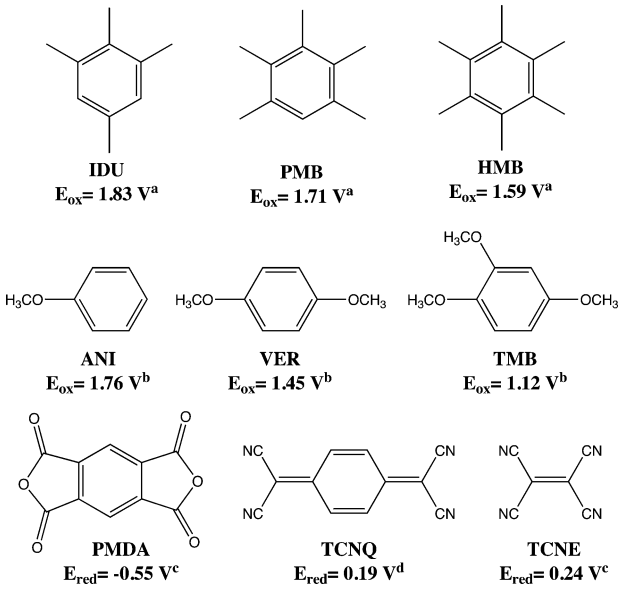

It will be shown that the observation of a weak but distinct excitation wavelength effect requires very specific conditions related not only to the chemical system (DAC and solvent) but also to the experimental parameters.

Experimental Section

Apparatus. The CR dynamics of excited DACs has been measured using both transient absorption (TA) and multiplex transient grating (TG).[42] Excitation at 400 nm was achieved with the frequency doubled output of a standard 1 kHz amplified Ti:Sapphire system (Spectra−Physics). The duration of the pulses was around 100 fs. Excitation between 480 and 620 nm was performed with a two-stage noncollinear optical parametric amplifier (NOPA, Clark−MXR). After recompression with a pair of prisms, the pulse duration was of the order of 45 fs.

The general layout of the TA setup has been described in detail elsewhere.[13] For these measurements, excitation was performed with the NOPA pulses and probing was carried out at 400 nm.

The multiplex TG setup has been described in detail previously.[8] Excitation was either at 400 nm or in the 480−620 nm range and probing was achieved with a white light continuum obtained by focusing 800 nm pulses in a H_2O/D_2O mixture. All TG spectra were corrected for the chirp of the probe pulses.

For both experiments, the energy of the pump pulses on the sample was around 250 nJ and the polarization of the probe light was at magic angle relative to that of the pump pulses. The width of the response function of both TA and TG experiments depended on the pump and probe pulses used but was less than 200 fs.

Samples. The electron acceptors pyromellitic dianhydride (PMDA, Aldrich), tetracyanoethylene (TCNE, Aldrich), and tetracyanoquinodimethane (TCNQ) were recrystallized and sublimed. The electron donors isodurene (IDU), anisole (ANI), veratrol (VER), 1,2,4-trimethoxybenzene (TMB), and *N*,*N*-diethylaniline (DEA) were vacuum distilled, while pentamethylbenzene (PMB) and hexamethylbenzene (HMB) were recrystallized. The solvents valeronitrile (VaCN) and octanenitrile (OcCN) were purified as described in the literature,[43] while acetonitrile (ACN) was of spectroscopic grade and was used as

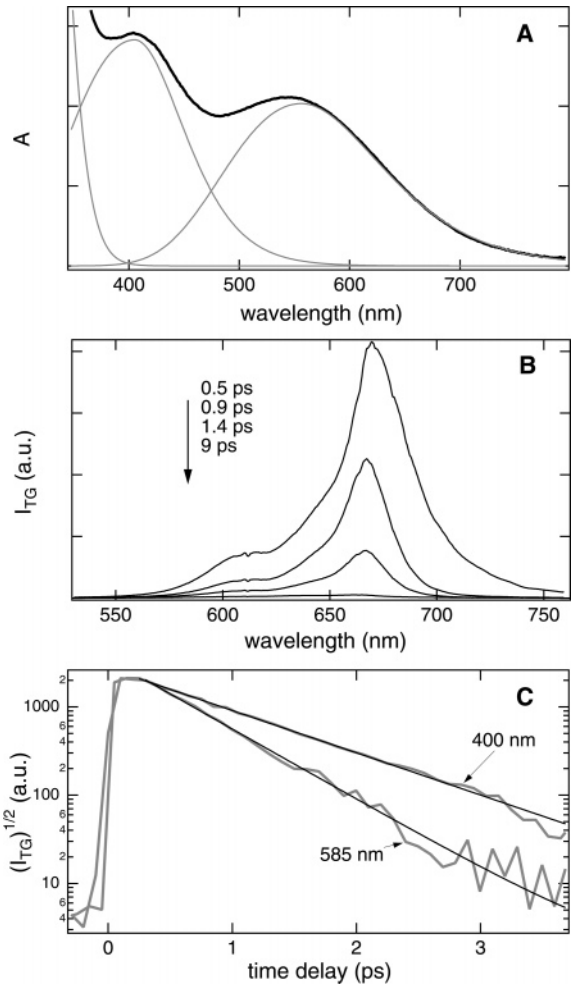

Figure 2. (A) Absorption spectrum of DEA/PMDA in ACN (thick line). Asymmetric Gauss functions used to reproduce the absorption spectrum (thin line). (B) TG spectra obtained at different time delays after excitation at 585 nm of DEA/PMDA in ACN. (C) Logarithmic plot of the time evolution of the square root of the TG intensity at 670 nm upon 400 and 585 nm excitation of DEA/PMDA in ACN (gray) and best single-exponential fits (black).

such. Unless specified, all compounds were from Fluka. The concentration of the acceptors was of the order of 0.15 M and that of the donors was adjusted to obtain an absorbance between 0.2 and 0.5 on 1 mm, the sample thickness, at the excitation wavelength. This corresponds to a stoichiometric excess of acceptor and minimizes the formation of 2:1 complexes.[35] During the experiments, the samples were continuously stirred by N_2 bubbling. No significant sample degradation was observed after the measurements.

Results

Complexes with PMDA. Figure 2A shows the steady-state absorption spectrum of a mixture of DEA and PMDA in ACN. This spectrum is characterized by two CT bands, designed as CT1 (lower energy) and CT2 (higher energy), which have been reproduced by asymmetric Gauss functions as described in ref 32. This simple line shape analysis was carried out to estimate the contribution of each CT band to the absorption spectrum, a more quantitative analysis[44,45] going beyond the scope of this study. The absorption maxima of the CT bands are listed in Table 2.

Figure 2B shows TG spectra measured at different time delays after excitation at 585 nm of the same complex in ACN. At this wavelength, excitation occurs essentially through the CT1 transition.

TABLE 2: CT Absorption Maxima, λ_{max} in nm, in ACN[a]

DAC	λ_{max} (CT1)	λ_{max} (CT2)
DEA/PMDA	556	405
TMB/PMDA	468	341
IDU/TCNQ	shoulder	
PMB/TCNQ	488	
HMB/TCNQ	534	
ANI/TCNQ	shoulder	
IDU/TCNE	465	
PMB/TCNE	492	
HMB/TCNE	520	
ANI/TCNE	486	373
VER/TCNE	569	418
TMB/TCNE	655	434

[a] These values are almost unchanged in VaCN and OcCN.

The nature of a TG spectrum has been described in detail elsewhere.[42] In brief, the TG intensity is proportional to the square of the photoinduced absorption and refractive index changes. The TG spectrum corresponds thus to the sum of the square of the transient absorption and dispersion spectra. In practice, it is very similar to the corresponding TA spectrum, the major difference being that it is always positive. The major advantage of TG over TA is its superior sensitivity due to the zero-background nature of the signal.

However, at time delays where the pump and probe pulses overlap, the TG signal contains an additional contribution due to the optical Kerr effect (OKE) in the solvent.[8] In this case, the TG intensity is given by:

$$I_{TG} = c_1 \Delta A_p^{\,2} + c_2(\Delta n_p + \Delta n_{OKE})^2 \qquad (1)$$

where c_1 and c_2 are constants, ΔA_p and Δn_p are the modulation amplitudes of absorbance and refractive index due to population changes, and Δn_{OKE} is the modulation amplitude of refractive index due to OKE. This nonresonant contribution interferes with the signal due to population changes through the cross term $2\Delta n_p \Delta n_{OKE}$ and because of this, the TG spectrum differs strongly from the TA spectrum. Consequently, the TG spectra recorded at time delays shorter than about 300 fs were discarded.

At longer time delays, the TG spectrum consists of an intense band centered at 670 nm with a shoulder around 610 nm. This band can be unambiguously ascribed to the $PMDA^{\bullet-}$ radical anion.[19,46,47] The $DEA^{\bullet+}$ radical cation has been reported to absorb weakly around 475 nm, i.e., out of the spectral window of the TG experiment (500−750 nm). Some spectral dynamics, blue-shift and band narrowing, can be observed. As discussed in detail in ref 25, these effects seem to be essentially related to some structural changes following CT excitation.

The same TG spectra are observed when exciting the complex at 400 nm, i.e., in CT2, the high-frequency CT band. Although the spectral features are the same at both excitation wavelengths, the decay dynamics of the TG band differ substantially. Figure 2C shows the decays of the square root of the TG intensity at 670 nm obtained upon CT1 and CT2 excitation. As the intensity maximum near time zero contains contributions from the Kerr effect, these time profiles were not analyzed by iterative reconvolution with the instrumental response function and only the decaying part of the time profile was considered. Figure 2C shows that these decays can be reasonably well reproduced with an exponential function. From this analysis, the time constant of CR, τ_{CR}, amounts to 550 fs upon CT1 excitation while it is equal to 900 fs when exciting in the CT2 band (see Table 3).

The CR dynamics has also been measured after excitation at 530 nm, i.e., at higher energy in the CT1 band. No significant difference could be observed compared with 585 nm excitation.

TABLE 3: CR Time Constants, τ_{CR}, Obtained from the Analysis of the Excited-State Population Decay of DACs Containing PMDA and TCNQ in Various Solvents and at Several Excitation Wavelengths, λ_e (limit of error on τ_{CR}: ±8%)

DAC	solvent	λ_e (nm)	τ_{CR} (ps)
DEA/PMDA	ACN	400	0.90
		530, 585	0.55
	VaCN	400	1.97
		550, 585	1.55
TMB/PMDA	ACN	400	0.34[a]
	VaCN	400	1.0
		515	0.75
		550	0.69
IDU/TCNQ	ACN	530	1.70
	VaCN	530	5.55
PMB/TCNQ	ACN	530	1.0
	VaCN	490, 530, 580	3.7
HMB/TCNQ	ACN	530	0.55
ANI/TCNQ	ACN	530	0.80

[a] Ref 25.

The signature of nonequilibrium CR dynamics is its nonexponential character. This effect should mainly show up at an early time, which in the present measurements is partially hidden by the nonresonant contribution from the solvent. Therefore, an excitation wavelength dependence of the early CR dynamics cannot be excluded.

The same measurements were repeated in VaCN, which is characterized by a slower dielectric response (see Table 1). The TG spectra exhibit the same features as in ACN. Although the decay dynamics are substantially slower, a qualitatively similar excitation wavelength effect is observed. Indeed, the CR time constant upon CT2 excitation is substantially slower than upon CT1 excitation (see Table 3). Moreover, it is essentially the same after 550 and 585 nm excitation.

Similar measurements have also been performed with the TMB/PMDA system in VaCN, which also exhibits two CT absorption bands (Figure 3A). Excitation at 400 nm occurs predominantly through the CT2 transition and the decay of the resulting ion pair population is markedly slower than upon CT1 excitation (see Table 3) as observed with DEA/PMDA. In this case however, a very small effect of the excitation wavelength was observed in the CT1 band as shown in Figure 3B. The amplitude of the small rise of the TG intensity after the OKE spike depends on the probe wavelength, indicating that this feature is essentially due to the interference between population and OKE. The time profiles were analyzed using a biexponential function but only the component with positive amplitude, i.e., the decaying part of the signal, was considered. The corresponding time constants are listed in Table 3. The small difference of decay time upon excitation at 550 and 515 nm is close to the limit of error (±8%) but is reproducible. In ACN, the dynamics is much faster and cannot be determined accurately enough with the TG technique because of the interference effect. A CR time constant of 340 fs has been measured by transient absorption with 400 nm excitation.[25]

Complexes with TCNQ. As nonequilibrium dynamics and excitation wavelength dependence are only expected when the time scale for CR is similar or shorter than that of solvation, the excited-state dynamics of several DACs containing TCNQ and various donors have first been investigated upon excitation at a fixed wavelength. The absorption spectra of these DACs consist of a single broad band, which appears as a shoulder with the weakest donors (see Table 2).

Figure 4A shows the TG spectrum measured 1 ps after excitation at 530 nm of IDU/TCNQ in ACN. This spectrum

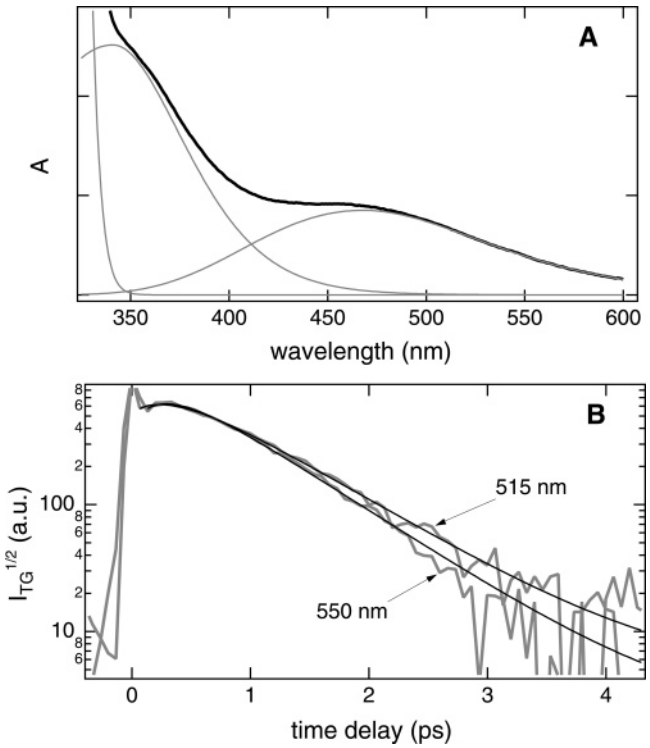

Figure 3. (A) Absorption spectrum of TMB/PMDA in ACN (thick line). Asymmetric Gauss functions used to reproduce the absorption spectrum (thin line). (B) Logarithmic plot of the time evolution of the square root of the TG intensity at 670 nm upon 515 and 550 nm excitation of TMB/PMDA in VaCN (gray) and best biexponential fits (black).

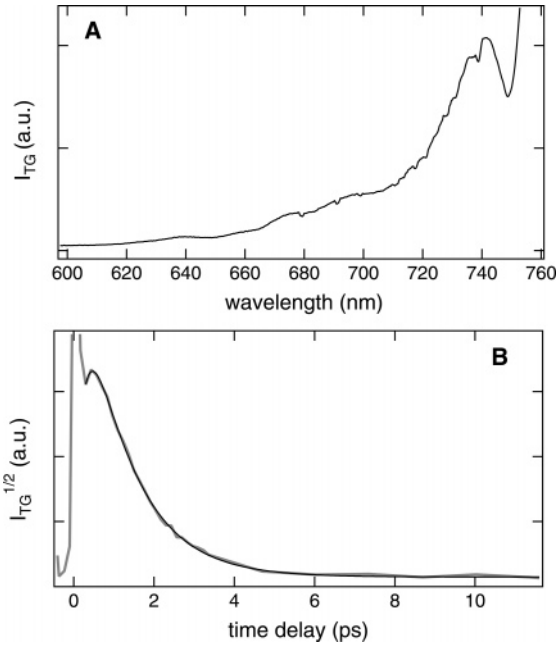

Figure 4. (A) TG spectrum measured 1 ps after excitation at 530 nm of IDU/TCNQ in ACN. (B) Time profile of the square root of the TG intensity at 740 nm upon 530 nm excitation of IDU/TCNQ in ACN (gray) and best biexponential fit (black).

can be safely ascribed to the $TCNQ^{\bullet -}$ radical anion.[46] For these measurements, a 600 nm cutoff filter was used to eliminate the scattered excitation light and therefore the $IDU^{\bullet +}$ cation cannot be observed. Similar TG spectra have been obtained with all the other donors investigated. Figure 4B shows the time profile of the square root of the TG intensity at 740 nm measured with IDU/TCNQ. Apart from the initial spike, this profile can be

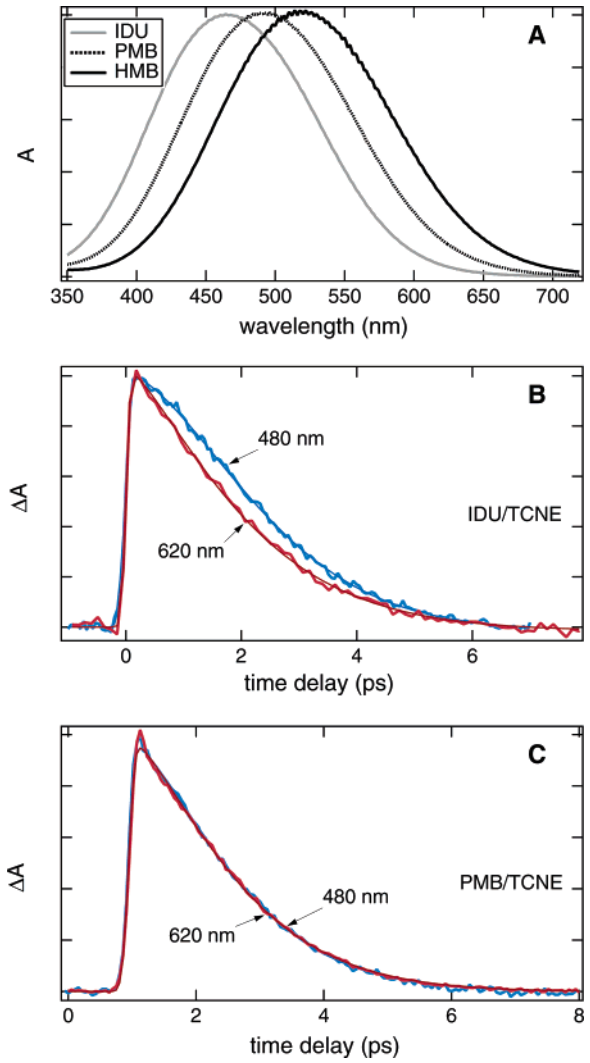

Figure 5. (A) Absorption spectra measured with TCNE and three methylbenzenes in ACN. (B) Time profiles of the transient absorption at 400 nm after excitation of IDU/TCNE at 480 and 620 nm in VaCN (thick blue and red lines) and best fits of eq 2 (thin lines). (C) Same as (B) but with PMB/TCNE.

well reproduced with a biexponential function. In this case again, only the time constant of the decaying component has been considered. The corresponding CR time constant is listed in Table 3 together with those obtained with other donors in ACN and in VaCN. The effect of excitation wavelength was investigated with PMB/TCNQ in VaCN, for which the CR dynamics is faster than that of diffusional solvation. The CR time constant upon excitation at 490 and 580 nm was the same, within the limit of error, as that measured with 530 nm excitation.

Complexes with TCNE. In a first stage, relatively weak donors such as methylbenzenes (MeB) have been used. The absorption spectra of MeB/TCNE mixtures exhibit a single broad absorption band with the maximum correlated with the redox potentials of the donor (see Table 2 and Figure 5A). To avoid interference effects associated with OKE, and thus, to be able to monitor the early time evolution of the excited-state population, the time dependence of the absorbance of $TCNE^{\bullet-}$ radical anion at 400 nm was measured by transient absorption. Figures 5B,C show time profiles of the TA at 400 nm measured with IDU/TCNE and PMB/TCNE in VaCN after excitation at 620 and 480 nm. Although the IDU/TCNE complex exhibits some absorption at this wavelength, its absorption coefficient is too small compared to that of $TCNE^{\bullet-}$ to contribute significantly to the transient signal.[41] With the stronger donors, the absorbance at 400 nm is negligibly small.

TABLE 4: Nonexponentiality Factor, *s*, Obtained from the Fit of Eq 2 to the Decay of the Excited State Population of TCNE Containing DACs in Various Solvents and at Several Excitation Wavelengths, λ_e and Effective CR Time Constants, τ_{eff} (Limit of Error on τ_{eff}: ±5%)

DAC	solvent	λ_e (nm)	*s*	τ_{eff} (ps)
IDU/TCNE	ACN	480, 530, 620	1.3	0.80
	VaCN	480	1.57	2.42
		530	1.53	2.25
		620	1.30	2.03
	OcCN	480	1.46	5.52
		530	1.35	5.14
		620	1.28	5.04
PMB/TCNE	ACN	480, 530 620	1.3	0.55
	VaCN	480, 530, 620	1.35	1.95
	OcCN	480, 530, 620	1.25	3.8
HMB/TCNE	ACN	480, 530, 620	1.3	0.45
	VaCN	480	1.31	1.35
		530	1.26	1.39
		620	1.19	1.46
	OcCN	480, 530, 620	1.17	2.65
ANI/TCNE	ACN	480, 530, 620	1.2	0.45
	VaCN	480	1.45	1.61
		530	1.30	1.53
		620	1.15	1.40
	OcCN	480	1.3	2.60
		530	1.3	2.55
		620	1.1	2.24
VER/TCNE	ACN	480, 530, 620	1	~0.12[a]
	VaCN	480, 530, 620	1.1	0.37
		480, 530, 620	1	0.5
TMB/TCNE	ACN	480, 530, 620	1	<0.1[a,b]
	VaCN	480, 530, 620	1	~0.14[a]
	OcCN	480, 530, 620	1	0.18

[a] Smaller than the instrument response function. [b] Biphasic decay at 480 and 530 nm excitation (see text).

Contrarily to the TG measurements, the TA profiles are free from interference and can be analyzed by iterative reconvolution of the instrument response function with a trial function. All decays could be well reproduced using the following trial function:

$$f(t) = A \exp[-(t/\tau)^s] \qquad (2)$$

This function with $s < 1$ is the stretch exponential function. It is widely used to describe systems exhibiting relaxation occurring in a large range of time scales.[48] However, the best fits shown in Figure 5 have been obtained with $s > 1$. This corresponds to a situation where the decay rate increases with time. This effect is particularly evident with IDU/TCNE excited at 480 nm, where the time profile after the initial rise remains almost constant for a few hundreds of femtoseconds. After about 2−3 ps the decay is close to exponential. As shown in Figure 5B, the CR dynamics depends clearly on the excitation wavelength with IDU/TCNE in VaCN. With HMB/TCNE (not shown) only a very weak effect is observed, while with PMB/TCNE, the CR dynamics is essentially independent of the excitation wavelength, at least between 480 and 620 nm. The *s* values obtained from the fit are listed in Table 4 together with the effective time constants, τ_{eff}, defined as:

$$\tau_{eff} = \frac{1}{\Delta A_{max}} \int_0^\infty \Delta A(t)\, dt \qquad (3)$$

where ΔA_{max} is the maximum signal intensity.

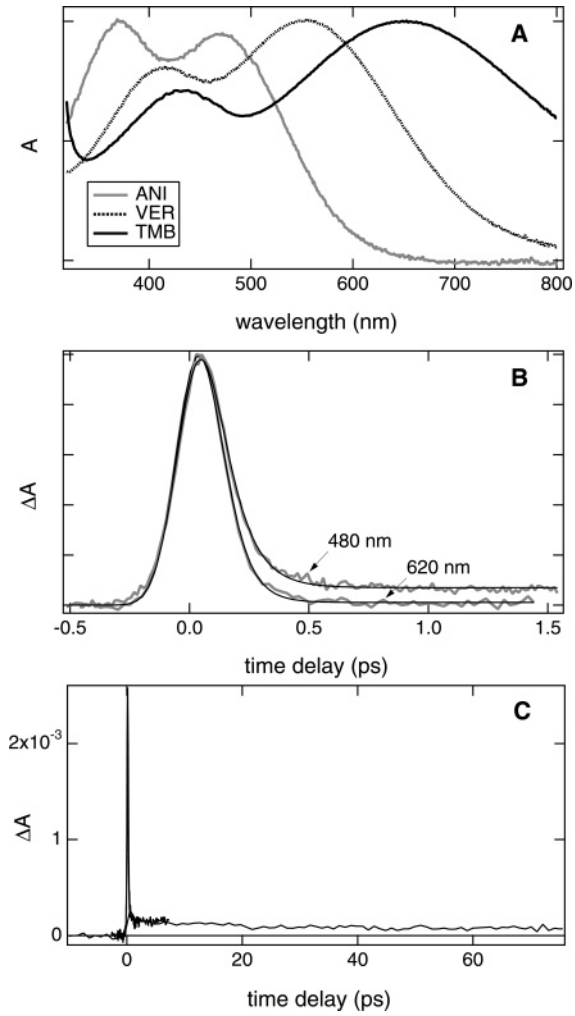

Figure 6. (A) Absorption spectra measured with TCNE and three methoxybenzenes in ACN. (B) Time profiles of the transient absorption at 400 nm after excitation of TMB/TCNE at 480 and 620 nm in ACN (gray) and best exponential fits (black). (C) Same as (B) but after 530 nm excitation.

The CR dynamics of these three DACs has also been measured in ACN and in OcCN. In ACN, the time profiles of the transient absorption are less nonexponential with *s* of the order of 1.3. Moreover, the CR dynamics is about three times as fast as in VaCN. However, no significant effect of the excitation wavelength can be observed even with IDU/TCNE. In OcCN, the CR dynamics is substantially slower than in VaCN. Although a small excitation wavelength dependence can be observed with IDU/TCNE, it is not as marked as in VaCN. With the other DACs, CR is essentially independent of the excitation wavelength.

Several complexes composed of TCNE and methoxybenzene derivatives (MoB) have also been investigated. With ANI, VER, and TMB as donors, two distinct CT absorption bands are observed (see Figure 6A).[34] In the presence of oxygen, a band which is very similar to that of $TCNE^{\bullet-}$ but lacks its characteristic vibrational structure, is also present. This effect is well documented and has been ascribed to the formation of the tricyanoethanolate anion.[49−51]

Figure 6B shows the time profile of the TA at 400 nm measured with TMB/TCNE in ACN with two different pump wavelengths, which coincide predominantly with the CT1 transition. After 620 nm excitation, the whole signal decays to zero within the response function of the instrument. The CR time constant can be estimated to be of the order of 50−80 fs. After 480 nm excitation, the decay is biphasic with an ultrafast component as measured with 620 nm excitation and a smaller slow component, which remains constant within the time window of the experiment (100 ps). As shown in Figure 6C, this "plateau" can still be observed upon 530 nm excitation, but its amplitude is smaller. This biphasic decay dynamics is no longer observed with the weaker donors, VER and ANI. With both donors, the dynamics is independent of the excitation wavelength, at least between 480 and 620 nm.

In VaCN and OcCN, the TA decay measured with TMB/TCNE is no longer biphasic even upon 480 nm excitation. In these two solvents, the CR dynamics is substantially slower than in ACN and does not exhibit any significant excitation wavelength dependence between 480 and 620 nm. The same behavior has been observed with VER/TCNE.

By contrast, the excited-state population dynamics of ANI/TCNE in VaCN and OcCN exhibits a small but reproducible wavelength dependence. As for IDU/TCNE, both the degree of nonexponentiality and the effective CR time constant increase by going from red to blue excitation. The effective decay times are listed in Table 4.

Discussion

The above results indicate that a dependence of the CR dynamics on the excitation wavelength is observed in a few cases only. Moreover, these cases can be sorted into three groups: (a) wavelength effects independent of the dynamic properties of the solvent, i.e., present in both ACN and VaCN, (b) effects measured in ACN only, and (c) effects appearing only in slower relaxing solvents, i.e., in VaCN and OcCN. These three groups of wavelength dependence have most probably different origins that are discussed below.

(a) Solvent-Independent Wavelength Effects. These effects have been observed with the two D/PMDA DACs. Indeed, CR upon CT2 excitation is in both cases and in both ACN and VaCN markedly slower than after CT1 excitation. The presence of two CT bands is typical for complexes with substituted benzenes as donor.[52] Upon substitution, the two highest occupied molecular orbitals (HOMO) of benzene are no longer degenerate and, therefore, the two CT bands correspond to transitions from the highest (HOMO) and the second highest (HOMO-1) occupied orbitals of the donor to the lowest unoccupied orbital (LUMO) of the acceptor. A substantial oscillator strength of a CT transition requires some overlap between donor and acceptor orbitals. For this reason, it has been suggested that the two CT bands correspond to DACs with different geometries, each of them favoring the overlap of either HOMO or HOMO-1 with the LUMO of the acceptor.[34] Consequently, a variation of CR dynamics upon CT1 and CT2 excitation is not really astonishing.

A major difference between CR from CT1 and CT2 is the driving force, ΔG_{CR}. For CR after CT1 excitation, it can be expressed as:

$$\Delta G_{CR1} = -E_{ox}(D) + E_{red}(A) - \frac{0.56\ \text{eV}}{\epsilon_s} \qquad (4)$$

where $E_{ox}(D)$ and $E_{red}(A)$ are the oxidation and reduction potentials of the donor and acceptor in acetonitrile, respectively, and ϵ_s is the static dielectric constant of the solvent. This relationship, based on an expression proposed by Weller,[53] was established for the xylene/tetracynobenzene DAC,[54] and can be expected to be valid for the complexes investigated here. Moreover, in polar solvents, the last term on the rhs of this equation is almost negligible. On the other hand, assuming that

the reorganization energy for both complexes is the same,[55] the driving force for CR from the CT2 state can be estimated from the following relation:

$$\Delta G_{CR2} - \Delta G_{CR1} = -h\Delta\nu_{CT} \quad (5)$$

where $\Delta\nu_{CT}$ is the frequency difference of the two CT band maxima. Alternatively, the difference between the second and first ionization potentials of the donor could be used instead of $h\Delta\nu_{CT}$. For the D/PMDA systems investigated here, the difference in driving force can be estimated to be about 0.9 eV (see Table 2).

The driving force dependence of the ultrafast CR dynamics of excited DACs has been shown to be weaker than predicted by the semiclassical theory of nonadiabatic ET reactions.[14,15,18,25] When represented on a logarithmic scale, the rate constant of CR increases almost linearly with decreasing exergonicity. For MoB/PMDA complexes, the slope of the free energy dependence amounts to 1.34 decade/eV.[25] Consequently, a 0.9 eV increase of exergonicity should result in a 16-fold decrease of CR rate constant. This is much larger than the decrease by a factor of about 1.5 observed here (see Table 3). Differences in the reorganization energy, λ, and/or in the electronic coupling matrix element, V, for CR from CT1 and CT2 could, in principle, counterbalance the effect of driving force. However, large differences in λ can reasonably be excluded because even if CT1 and CT2 are due to complexes with different geometries, they are composed of the same molecules.

To counterbalance the difference of driving force, the coupling constant V for CR from the CT2 state should be larger than that for CR from the CT1 state by a factor 3.2. The magnitude of V can, in principle, be deduced from the dipole moments of the two transitions. According to Voigt and co-workers,[56] the two CT bands of complexes with TCNE and substituted benzenes have essentially the same oscillator strength. One can thus expect a similar trend with PMDA.

One possible explanation for the weak difference of CR dynamics is that the DACs do not have very precise geometries where the overlap between the LUMO of the acceptor with either the HOMO or the HOMO-1 of the donor vanishes. As shown by Voigt and co-workers,[56] the ratio of the area of the two CT absorption bands is temperature dependent above 200 K, indicating equilibrium between the DACs geometries. In most cases, the overlap with both donor orbitals must be substantial and, consequently, the oscillator strength for both CT transitions should be simultaneously nonzero. Therefore, the CT2 band can be thought of as being due to a transition to an upper excited state of the complex. After internal conversion to CT1, CR with ΔG_{CR1} takes place. In principle, CR from the CT2 state is also possible but, due to its larger driving force, it can be expected to be much slower than internal conversion to CT1. Thus CR always occurs from CT1, independently of the excitation wavelength.

The observed wavelength effect on the CR dynamics can be explained in terms of different DAC geometries and by considering that there is no geometry where the orbital overlap is simultaneously optimal for both CT1 and CT2. DACs with a geometry favoring the coupling with the HOMO-1 and, hence, with a relatively small V for CR (V_-) have a higher absorption coefficient of the CT2 band. On the other hand, DACs with a configuration favoring the coupling with the HOMO and which have thus a larger V for CR (V_+) have a higher absorption coefficient of the CT1 band. Therefore, CR after CT2 excitation is slower than upon CT1 excitation. Considering the time scale of CR, the geometry of the excited DAC can be considered as frozen and changes of configuration in the excited state can thus be safely neglected.

As the rate constant of CR is proportional to V^2, the observed ratio of rate constants k_{CR1}/k_{CR2} is reproduced with a V_+/V_- ratio of about 1.25 only. Therefore, a rather narrow distribution of DAC geometries is sufficient to account for this effect.

This wavelength effect observed with TMB/PMDA and DEA/PMDA has probably little to do with nonequilibrium dynamics. This explains why it is observed in both ACN and VaCN, which have very different dynamic properties.

(b) Wavelength Effects Observed in ACN Only. The absorption spectrum of TMB/TCNE in Figure 6A shows that 620 nm excitation pulses interact essentially with the CT1 transition, while 530 and especially 480 nm excitation pulses interact partially with the CT2 transition. Therefore, if we assume different DAC geometries as just discussed above, the coupling constant for CR upon blue excitation should be smaller than for CR after red excitation. Another peculiarity of the TMB/TCNE complex is its small driving force for CR, i.e., $\Delta G_{CR1} = -0.88$ eV. Although the total reorganization energy, λ, for CR in such complexes is not known, it is not unrealistic to think that $-\Delta G_{CR1} < \lambda$, and therefore, CR should, in principle, occur in the so-called normal regime. As shown in Figure 7, CR from the equilibrated excited DAC is thermally activated and can be expected to be slow. However, if the coupling constant V is sufficiently large, hot charge recombination can occur in parallel to relaxation. If CR occurs only partially during relaxation, the decay of the excited-state population should be biphasic with an ultrafast component due to hot CR and a slow component due to thermal CR. This could be an explanation for the biphasic decay shown in Figure 6.

The wavelength effect could now be related to the variation of V with excitation wavelength. V is the largest for red excitation, and in this case CR occurs totally before equilibrium has been reached. With blue wavelength, DACs with smaller V are excited. For this subpopulation, the hot CR is not complete and thus a fraction of the excited-state population relaxes to the equilibrium from where it recombines thermally. Hence, the biphasic decay is only observed at short excitation wavelength.

The absence of biphasic decay in VaCN and OcCN can be explained by the slower relaxation times of these solvents, which favor nonequilibrium CR even with relatively smaller V values.

Finally, the absence of biphasic decay with other donors can be explained by the larger driving force for CR, i.e., $\Delta G_{CR1} = -1.21$ eV for VER/TCNE. With VER and ANI, CR occurs essentially in the barrierless or the inverted regime and is thus not a thermally activated process.

A biphasic decay of the ion pair population generated upon electron-transfer quenching of perylene by TCNE has recently been reported.[13] It was shown that more than 95% of the ion pair population undergoes ultrafast CR, most probably hot CR, while the remaining fraction undergoes slow CR as expected for the normal, thermally activated regime.

(c) Wavelength Effects Observed in Slower Relaxing Solvents Only. The gradual slowing down of CR dynamics with decreasing excitation wavelength, accompanied by an increase of the nonexponential character, has been observed with a few DACs only and in the slower solvents, but not in ACN.

This wavelength effect is most probably due to the nonequilibrium nature of the CR (see Figure 1). It is indeed only observed when the effective CR time constant is shorter than that of diffusive solvation. Indeed, in the case of IDU/TCNE, the wavelength effect is substantial in VaCN, where the CR time constant is of the order of 2 ps and the solvation time is

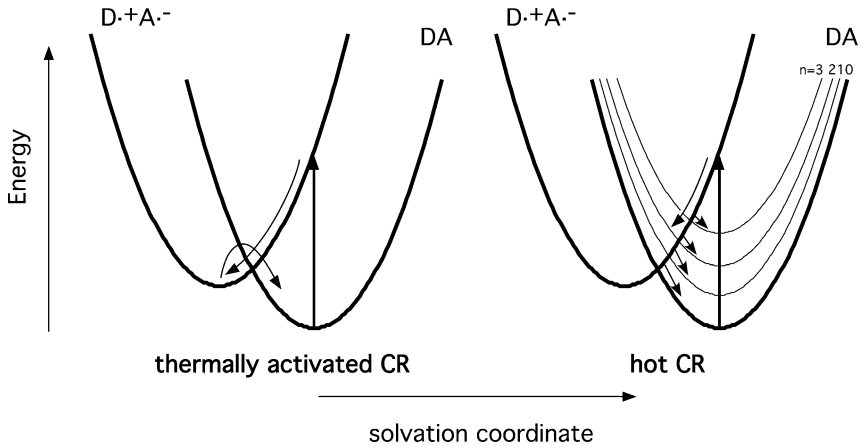

Figure 7. Illustration of thermally activated and hot CR pathways using cuts in the free energy surface of the ground and excited states of a DAC along the solvation coordinate.

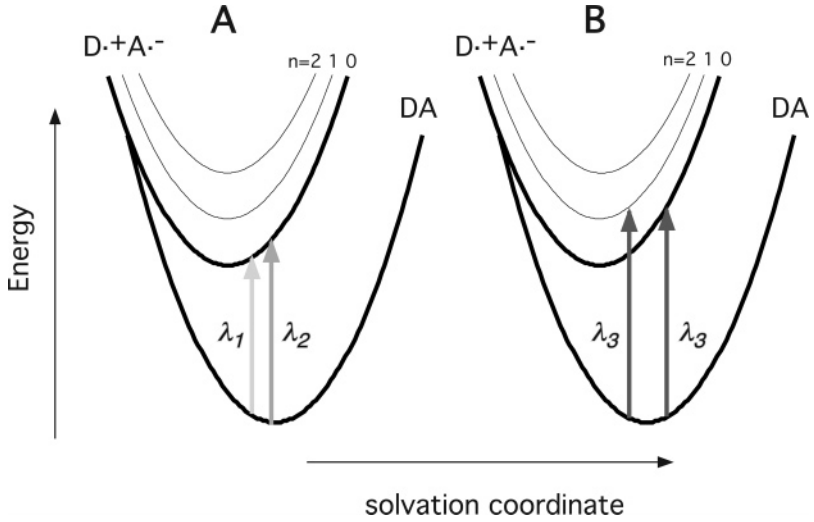

Figure 8. Illustration of the correlation between the excitation wavelength and the initial location of the excited-state population on the solvation coordinate. (A) With red edge excitation (λ_1 and λ_2), only the lower vibrational state ($n = 0$) of the electronic excited state is populated. (B) With shorter excitation wavelength (λ_3), several vibrational states of the electronic excited states ($n = 0, 1$) can be populated at various locations on the solvation coordinate.

4.7 ps. The effect is less marked in OcCN, where the CR time constant is around 5.5 ps and the solvation time is 6.4 ps. The relatively large increase of the CR time constant when going from VaCN to OcCN is most probably related to the smaller polarity of the latter.

Finally, no effect was measured with these DACs in ACN where CR is slower than solvation. The nonexponential character of the decay, quantified here by *s*, and its increase with increasing excitation energy are also typical for nonequilibrium dynamics as shown by recent simulations using various theoretical models.[29−31]

The broad absorption band of IDU/TCNE is in fact due to two nearly degenerate CT transitions,[32,57] originating from the splitting of the two highest occupied molecular orbitals of IDU as discussed above. As this splitting is very small, both transitions have almost the same probability to be excited in the wavelength range investigated. Therefore, the presence of these two CT states should not lead to a significant excitation wavelength dependence. This is confirmed by the fact that the measured wavelength effect is strongly solvent dependent. Moreover, it is also observed with ANI/TCNE using pump wavelengths interacting with the CT1 transition only.

With donors stronger than IDU and ANI, the CR dynamics is substantially faster but the excitation wavelength dependence is much weaker or insignificant. The absorption spectra of IDU/TCNE and ANI/TCNE show that the longer excitation wavelength used, i.e., 620 nm, corresponds to the onset of the CT band. With the stronger donors, this wavelength is closer to the band maximum. Resonance Raman measurements with HMB/TCNE indicate the presence of many Franck−Condon active vibrational modes associated with the CT transition.[35,58] Therefore, excess excitation energy is deposited not only in the solvent modes but also in the vibrational modes. As shown in Figure 8A, a correlation between the excitation wavelength and the solvation coordinate only exists at long wavelengths (λ_1 and λ_2). Excitation at shorter wavelengths (λ_3 in Figure 8B) populates various vibrational excited states at different locations on the solvation coordinate. After ultrafast relaxation to the vibrational ground state, the population is spread out over a wide range of positions on the solvation coordinate. Therefore, only a long excitation wavelength is able to bring the excited-state population into a rather localized position on the solvation coordinate. This is at the origin of the so-called "red-edge excitation" effect, which is observed with molecules characterized by a large difference in electric dipole moment between the ground and the excited state in rigid and polar media.[59−61] In these conditions, the fluorescence spectrum depends on the excitation wavelength on the red edge of the absorption band. At shorter excitation wavelength, the dependence vanishes or is much weaker.

Consequently, the excitation wavelength dependence observed with ANI/TCNE and IDU/TCNE can be considered to be a red-edge excitation effect on the CR.

It should be noted that in principle the nonexponentiality of the transient absorption decay could also be related to some spectral dynamics of the $TCNE^{\bullet-}$ absorption band, due for example to vibrational relaxation. Moreover, this spectral dynamics could be more important when exciting with more energy and could thus account for the observed excitation wavelength effect. However, if this process is at the origin of the wavelength dependence observed with ANI/TCNE and IDU/TCNE in VaCN and in OcCN, it is then difficult to explain its absence in ACN and with the other electron donors.

Braun and co-workers have recently reported measurements of the free ion yield following the excitation at different wavelengths of alkylbenzene/TCNE DACs in dichloromethane.[37] A more than 100-fold increase of the free ion yield was observed with PMB/TCNE by varying the excitation wavelength from 530 to 400 nm. This effect was ascribed to the excitation at short wavelength of "random donor−acceptor pairs", which are characterized by a relatively large separation distance (1 nm and more) and which absorb, although very weakly, predominantly on the blue side of the DAC CT band. This observation does not contradict the results discussed here. Indeed, in the present experiment, the time evolution of the whole excited-state population is monitored, while in ref 37, only the free ion population is detected using transient photoconductivity. In these experiments, the free ion yield was found to be extremely small, between 10^{-6} and 10^{-4}. Consequently, the contribution of the excited random donor−acceptor pair population to the transient absorption signal is negligibly weak and thus could not be observed here.

Conclusion

This investigation shows that for the excitation wavelength to have an effect on the CR dynamics of excited DACs, very specific conditions are required:

(1) If the complex exhibits two well-separated CT bands, CR following excitation of the high-energy transition is slower than after excitation in the low-energy transition. This effect is apparently mostly related to the relative geometries of the complexes. DACs, with a geometry favoring a large oscillator strength of the high-energy CT transition, have a smaller electronic coupling constant for CR than DACs with a geometry enabling a large oscillator strength of the low-energy CT transition.

(2) If the driving force for CR is small, the relative contribution of two CR pathways, namely hot (or nonequilibrium) and thermally activated, can apparently be changed by exciting in different CT bands.

(3) If CR takes place within a shorter time scale than diffusive solvation, a slowing down of the CR dynamics with increasing excitation energy can be observed if the experiment is performed in the red edge of the CT absorption band.

The effect of excitation wavelength is, therefore, an interesting tool to obtain information on the nature of DACs. The dynamics of weakly exergonic CR is particularly intriguing and should be investigated in more detail. These measurements indicate that DACs might be potential candidates for the demonstration of the coherent control of the dynamics of a chemical reaction in the condensed phase.

Acknowledgment. The authors wish to thank Anatoly Ivanov (University of Volgograd) for fruitful discussions. This work was supported by the Fonds National Suisse de la Recherche Scientifique through project no. 200020-107466/1.

References and Notes

(1) Mataga, N.; Miyasaka, H. *Adv. Chem. Phys.* **1999**, *107*, 431.
(2) Vauthey, E. *J. Phys. Chem. A* **2000**, *104*, 1804.
(3) Barbara, P. F.; Meyer, T. J.; Ratner, M. A. *J. Phys. Chem.* **1996**, *100*, 13148.
(4) Weller, A. *Pure Appl. Chem.* **1982**, *54*, 1885.
(5) Li, B.; Peters, K. S. *J. Phys. Chem.* **1993**, *97*, 7648.
(6) Hviid, L.; Brouwer, A. M.; Paddon-Row, M. N.; Verhoeven, J. W. *ChemPhysChem* **2001**, *2*, 232.
(7) Haselbach, E.; Pilloud, D.; Suppan, P. *Helv. Chim. Acta* **1998**, *81*, 670.
(8) Vauthey, E. *J. Phys. Chem. A* **2001**, *105*, 340.
(9) Gould, I. R.; Ege, D.; Moser, J. E.; Farid, S. *J. Am. Chem. Soc.* **1990**, *112*, 4290.
(10) Kikuchi, K. J. *Photochem. Photobiol. A* **1992**, *65*, 149.
(11) Brunschwig, B. S.; Ehrenson, S.; Sutin, N. *J. Am. Chem. Soc.* **1984**, *106*, 6858.
(12) Nicolet, O.; Vauthey, E. *J. Phys. Chem. A* **2003**, *107*, 5894.
(13) Pagès, S.; Lang, B.; Vauthey, E. *J. Phys. Chem. A* **2004**, *108*, 549.
(14) Asahi, T.; Mataga, N. *J. Phys. Chem.* **1989**, *93*, 6575.
(15) Asahi, T.; Mataga, N.; Takahashi, Y.; Miyashi, T. *Chem. Phys. Lett.* **1990**, *171*, 309.
(16) Asahi, T.; Mataga, N. *J. Phys. Chem.* **1991**, *95*, 1956.
(17) Marcus, R. A.; Sutin, N. *Biochim. Biophys. Acta* **1985**, *811*, 265.
(18) Hubig, S. M.; Bockman, T. M.; Kochi, J. K. *J. Am. Chem. Soc.* **1996**, *118*, 3842.
(19) Asahi, T.; Ohkohchi, M.; Mataga, N. *J. Phys. Chem.* **1993**, *97*, 13132.
(20) Gould, I. R.; Noukakis, D.; Gomez-Jahn, L.; Goodman, J. L.; Farid, S. *J. Am. Chem. Soc.* **1993**, *115*, 4405.
(21) Tachiya, M.; Murata, S. *J. Am. Chem. Soc.* **1994**, *116*, 2434.
(22) Frantsuzov, P. A.; Tachiya, M. *J. Chem. Phys.* **2000**, *112*, 4216.
(23) Walker, G. C.; Akesson, E.; Johnson, A. E.; Levinger, N. E.; Barbara, P. F. *J. Phys. Chem.* **1992**, *96*, 3728.
(24) Denny, R. A.; Bagchi, B.; Barbara, P. F. *J. Chem. Phys.* **2001**, *115*, 6058.
(25) Nicolet, O.; Vauthey, E. *J. Phys. Chem. A* **2002**, *106*, 5553.
(26) Jarzeba, W.; Pommeret, S.; Mialocq, J.-C. *Chem. Phys. Lett.* **2001**, *333*, 419.
(27) Wynne, K.; Galli, C.; Hochstrasser, R. M. *J. Chem. Phys.* **1994**, *100*, 4797.
(28) Wynne, K.; Reid, G. D.; Hochstrasser, R. M. *J. Chem. Phys.* **1996**, *105*, 2287.
(29) Ivanov, A. I.; Belikeev, F. N.; Fedunov, R. G.; Vauthey, E. *Chem. Phys. Lett.* **2003**, *372*, 73.
(30) Mikhailova, V. A.; Ivanov, A. I.; Vauthey, E. *J. Chem. Phys.* **2004**, *121*, 6463.
(31) Fedunov, R. G.; Feskov, S. V.; Ivanov, A. I.; Nicolet, O.; Pagès, S.; Vauthey, E. *J. Chem. Phys.* **2004**, *121*, 3643.
(32) Rossi, M.; Buser, U.; Haselbach, E. *Helv. Chim. Acta* **1976**, *59*, 1039.
(33) Hayashi, M.; Yang, T.-S.; Yu, J.; Mebel, A.; Lin, S. H. *J. Phys. Chem. A* **1997**, *101*, 4156.
(34) Voigt, E.-M. *J. Am. Chem. Soc.* **1964**, *86*, 3611.
(35) Smith, M. L.; McHale, J. L. *J. Phys. Chem.* **1985**, *89*, 4002.
(36) Markel, F.; Ferris, N. S.; Gould, I. R.; Myers, A. B. *J. Am. Chem. Soc.* **1992**, *114*, 6208.
(37) Zhou, J.; Findley, B. R.; Teslja, A.; Braun, C. L.; Sutin, N. *J. Phys. Chem. A* **2000**, *104*, 11512.
(38) Zhou, J.; Findley, B. R.; Braun, C. L.; Sutin, N. *J. Chem. Phys.* **2001**, *114*, 10448.
(39) Riddick, J. A.; Bunger, W. B. *Organic Solvents*; J. Wiley: New York, 1970.
(40) Gumy, J. C.; Nicolet, O.; Vauthey, E. *J. Phys. Chem. A* **1999**, *103*, 10737.
(41) Ganesan, V.; Rosokha, S. V.; Kochi, J. K. *J. Am. Chem. Soc.* **2003**, *125*, 2559.
(42) Högemann, C.; Pauchard, M.; Vauthey, E. *Rev. Sci. Instrum.* **1996**, *67*, 3449.
(43) Armagero, W. L. F.; Chai, C. L. L. *Purification of Laboratory Chemicals*; Elsevier: Amsterdam, 2003.
(44) Marcus, R. A. *J. Phys. Chem.* **1989**, *93*, 3078.
(45) Myers, A. B. *Chem. Phys.* **1994**, *180*, 215.
(46) Shida, T. *Electronic Absorption Spectra of Radical Ions*; Elsevier: Amsterdam, 1988; Vol. Physical Sciences data 34.
(47) Andruniow, T.; Pawlikowski, M. *Chem. Phys. Lett.* **2000**, *321*, 485.
(48) Edholm, O.; Blomberg, C. *Chem. Phys.* **1999**, *252*, 221.
(49) Spange, S.; Maenz, K.; Stadermann, D. *Liebigs Ann. Chem.* **1992**, *10*, 1033.

(50) Sakato, T.; Okai, T.; Tsubomura, H. *Bull. Chem. Soc. Jpn*. **1975**, *48*, 2207.
(51) de Boer, J. A. A.; Reinhoudt, D. N.; Viterwijk, J. W. H. M.; Harkema, S. *J. Chem. Soc. Chem. Commun.* **1982**, 194.
(52) Orgel, L. E. *J. Chem. Phys.* **1955**, *23*, 1352.
(53) Weller, A. Z. *Phys. Chem. N. F.* **1982**, *133*, 93.
(54) Arnold, B. R.; Farid, S.; Goodman, J. L.; Gould, I. R. *J. Am. Chem. Soc.* **1996**, *118*, 5482.
(55) Hush, N. S. *Prog. Inorg. Chem.* **1967**, *8*, 391.
(56) Mobley, M. J.; Rieckhoff, K. E.; Voigt, E.-M. *J. Phys. Chem.* **1977**, *81*, 809.
(57) Klessinger, M. *Angew. Chem., Int. Ed. Engl.* **1972**, *11*, 525.
(58) Kulinowski, K.; Gould, I. R.; Myers, A. B. *J. Phys. Chem.* **1995**, *99*, 9017.
(59) Itoh, K.-I.; Azumi, T. *Chem. Phys. Lett.* **1973**, *22*, 395.
(60) Funfschilling, F.; Zschokke-Gränacher, I.; Williams, D. F. *J. Chem. Phys.* **1981**, *75*, 3669.
(61) Fee, R. S.; Maroncelli, M. *Chem. Phys.* **1994**, *183*, 235.